IEEE Access
Multidisciplinary | Rapid Review | Open Access Journal

Received August 26, 2020, accepted September 11, 2020, date of publication September 15, 2020, date of current version October 1, 2020.

Digital Object Identifier 10.1109/ACCESS.2020.3024212

Dynamic Equivalent Modeling for Wind Farms With DFIGs Using the Artificial Bee Colony With K-Means Algorithm

XIAOHUI WANG[1,2], (Graduate Student Member, IEEE), HAO YU[3], YONG LIN[3], ZHEMENG ZHANG[1,2], (Graduate Student Member, IEEE), AND XIANFU GONG[3]

[1]College of Electrical and Information Engineering, Hunan University, Changsha 410082, China
[2]Hunan Key Laboratory of Intelligent Information Analysis and Integrated Optimization for Energy Internet, Hunan University, Changsha 410082, China
[3]Grid Planning and Research Center, Guangdong Power Grid Company, Ltd., Guangzhou 510080, China

Corresponding author: Hao Yu (yuhao1235813@163.com)

This work was supported by the National Natural Science Foundation of China under Grant 51722701.

ABSTRACT With the increasing penetration of wind power, it is recognized that wind power will have a greater and greater impact on the planning and operation of the original power system. And the detailed modeling of wind farm with doubly-fed induction wind generator (DFIG) will require large storage and computation resources, which poses technical challenges for equivalent modeling of wind farm. In this paper, a multi-machine dynamic equivalent modeling method for wind farms with DFIGs is proposed. First, the artificial bee colony with k-means (ABC-KM) algorithm is proposed to improve the effectiveness of wind farm clustering. Second, the operating data composed of wind speed, pitch angle, rotor angular velocity, rotor current, real-time active and reactive power are selected as clustering indicators. A wind farm with DFIGs is divided into several groups and DFIGs in the same group are clustered as one DFIG through equivalent parameter aggregation. The proposed wind farm modeling method consisting of clustering method and clustering indicators is verified by comparing the simulation results of equivalent and detailed models at steady-state and dynamic-state cases.

INDEX TERMS Dynamic equivalent model, wind farm with DFIG, clustering indicators, ABC-KM clustering algorithm, active prosumers.

I. INTRODUCTION

With the rapid development of wind power technology, the scale of grid-connected wind farms is gradually increasing. In 2019, 60.4 GW of wind energy capacity was installed globally with a growth of 19%, and the total capacity for wind energy globally has been over 651 GW by 2019. Wind energy, as a type of distributed energy resources (DERs), plays an important role in the energy transition from fossil fuels to renewable energy. And the growing penetration of DERs has made it possible for traditional passive consumers to evolve into active prosumers [1]. Therefore, the modeling methods, forecasting methods and related key technologies of DERs are still hot topics that require substantial scientific research [2]–[4]. And the modeling method for wind farms is mainly studied in this paper.

The associate editor coordinating the review of this manuscript and approving it for publication was Huai-Zhi Wang.

The existing methods on the modeling of wind farms with doubly-fed induction wind generator (DFIG) are divided into two categories of single-machine and multi-machine equivalent methods. The latter method represents wind farms by several equivalent DFIGs, which are obtained by clustering of indicators and equivalence of parameters [5]–[7]. In practice, the distribution of wind speed in large wind farms is not generally uniform, due to topography and wake effect issues, and DFIGs in the same wind farm often work at different operation states [8], [9]. Therefore, the multi-machine equivalent method can represent the more comprehensive dynamic characteristics of grid-connection wind farms.

Accordingly, the choice of clustering indicators is an important issue in the dynamic equivalent for wind farms. In [10], fault-front terminal voltage, fault-end terminal voltage, rotor speed, active power and reactive power were selected as clustering indicators. 13 variables were extracted as clustering indicators in [11] to describe the operation

This work is licensed under a Creative Commons Attribution 4.0 License. For more information, see https://creativecommons.org/licenses/by/4.0/

characteristics of DFIGs based on the voltage and flux equation analyses. A linear dynamic equivalent model for a wind farm was developed using measured data in [12]. In [13], long-time scale measured data was used as clustering indicators considering changing wind speeds in wind farms. The rotor speed vectors of wind turbines were sampled as clustering indicators under the combined conditions of different operating conditions and fault types in [14]. A dynamic multi-turbine multi-state model of wind farms was proposed based on historical wind data in [15]. Nevertheless, the above literature does not prove the effectiveness of the selected clustering indicators by comparison.

The choice of clustering method is another important issue in the dynamic equivalent for wind farms. A probabilistic clustering approach was proposed that determines equivalent number of wind turbines and the corresponding parameters in [16]. A multi-machine representation dynamic equivalent method based on the fuzzy C-means was proposed considering the active power characteristics of DFIGs in [17]. In [18], an improved support vector clustering approach was proposed for the single-wind condition dynamic aggregation of large wind farms. The geometric template matching based time series clustering method was developed for wind turbines in [19]. A clustering method was presented according to the slip coherency of wind turbines in [20].

The existing k-means (KM) algorithm is commonly used in the clustering analysis. However, it is sensitive to initial conditions and may consume a lot of calculation time due to the lack of stability in clustering [21]. In this paper, we propose a multi-machine dynamic equivalent modeling method for wind farms with DFIGs. The paper is organized as follows. In Section II, the model of DFIG is introduced, the artificial bee colony with k-means (ABC-KM) algorithm is developed, and the comprehensive indicators consisting of wind speed, pitch angle, rotor angular velocity, rotor current, real-time active and reactive power are selected as clustering indicators. In Section III, the equivalent parameters are calculated. The effectiveness of the proposed equivalent modeling method is illustrated in Section IV by comparing the simulation results of equivalent and detailed models with different clustering methods and clustering indicators both for steady-state and dynamic-state cases. Finally, the conclusions are drawn in Section V.

II. DYNAMIC EQUIVALENT MODELING FOR WIND FARM WITH DFIG

A. MODELING OF DFIG

The DFIG model shown in Figure 1 is comprised of the wind turbine, the gearbox, the induction generator and the converter. The stator side of DFIG is directly connected to the grid, and the rotor side of DFIG is connected to the grid through a back-to-back converter that handles only the slip power. The mathematical models of mechanical and electric systems of DFIG can be found in [22]. In this section, the modeling of the back-to-back converter consisting of rotor-side converter (RSC) and grid-side converter (GSC) is the main focus.

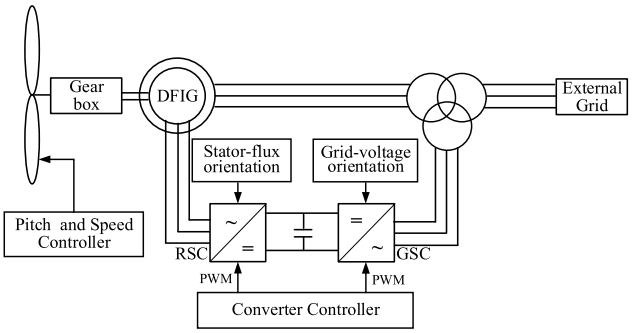

FIGURE 1. The overall model of DFIG.

1) ROTOR-SIDE CONVERTER

The rotor of induction generator can be excited by rotor-side converter for the decoupled control of active power and reactive power. The stator-flux orientation is used for the RSC control in which the stator flux is collinear with the d-axis.

2) GRID-SIDE CONVERTER

The direct-current capacitor's voltage can be controlled by grid-side converter which allows the reactive power flow for voltage stability. Furthermore, the power grid voltage orientation is used for the GSC control in which the grid voltage is collinear with the d-axis.

B. ABC-KM CLUSTERING ALGORITHM

The existing KM clustering algorithm is sensitive to initial conditions, which consumes massive time and loses the stability of clustering. Therefore, in order to improve the stability and effectiveness of clustering, ABC-KM algorithm combined with artificial bee colony algorithm and k-means algorithm is proposed in this paper.

In the algorithm proposed in this paper, the initial location of the honey source can be expressed as follows:

$$x_{ij} = x_{\min,j} + rand(0,1)(x_{\max,j} - x_{\min,j}) \tag{1}$$

where $x_{\max,j}$, $x_{\min,j}$ are the maximum and minimum of the jth dimension, respectively.

The new location of the honey source during the search can be expressed as follows:

$$v_{ij} = x_{ij} + \beta_{ij}(x_{ij} - x_{kj}) \tag{2}$$

where β_{ij} represents the random number in the interval $[-1, 1]$.

The fitness of honey source is expressed as follows:

$$fit_m(x_m) = \begin{cases} \dfrac{1}{1 + f_m(x_m)} \\ 1 + abs(f_m(x_m)) \end{cases} \tag{3}$$

where f_m is the function value corresponding to the m-th employed bee.

The probability based on the fitness obtained by employed bees for an onlooker bee to select the honey source is expressed as follows [23]:

$$P_i = \frac{fit(x_i)}{\sum_{n=1}^{SN} fit(x_n)} \tag{4}$$

Based on the proposed improvements in the ABC algorithm, the clustering center that corresponds to each bee is determined at the beginning of iteration, which can improve the stability and the calculation speed in the KM algorithm. The flow dagram of ABC-KM algorithm is shown in Figure 2 with the detailed procedure described as follows:

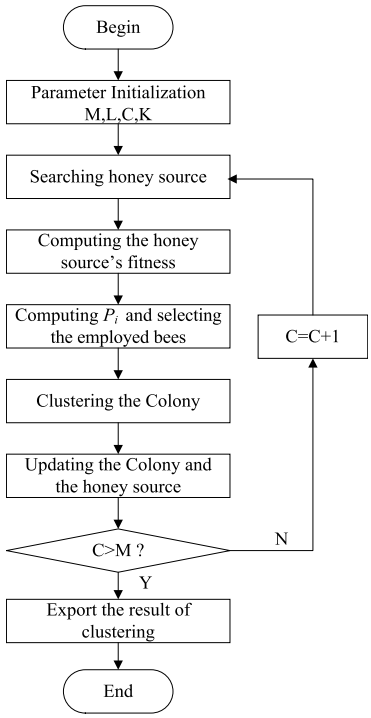

FIGURE 2. Flow diagram of ABC-KM algorithm.

1) Parameter initialization: Set the numbers for three kinds of bees, maximum iteration number M, control parameter L, and initial iteration number C = 1.
2) According to the fitness of bees, the bees are divided into two categories of employed and onlooker bees; a new honey source is generated according to (2).
3) Calculate the new honey source fitness and replace the original honey source if the new source has higher fitness.
4) Calculate P_i according to (4).
5) Select employed bees based on the greedy principle; onlooker bees search for the new honey source near the corresponding honey source.
6) Cluster the honey source with KM algorithm and update the bee colony after the search is done.
7) If the location is not updated after M iterations, the employed bees will transform into scout bees.
8) If C > M, go to step 9, otherwise, go to step 2 for the next round of calculations; set C = C + 1.
9) Export the clustering results.

C. CLUSTERING INDICATORS OF DFIG

1) WIND SPEED

The wind speed is an important factor in determining the output power of wind turbines, which can reflect the location of the wind turbine and interactions among multiple DFIGs considering the wake effect. Therefore, wind speed is selected as a clustering indication to distinguish different operating characteristics of DFIGs. Based on aerodynamic principles, the output power of wind turbine is stated as follows:

$$P_m = \frac{1}{2}\rho\pi R^2 C_P(\lambda, \beta)v_w^3 \tag{5}$$

where ρ is the air density, R is the wind turbine radius, v_w is the wind speed, C_p is the power coefficient with a set of nonlinear curves and the theoretical maximum is 0.593.

2) PITCH ANGLE

It can be seen from (5) that the power coefficient C_P will change when the pitch angle β changes, thereby affecting the output power of the wind turbine. The pitch angle also has a relationship with wind speed. When the wind speed is between cut-in and rated wind speeds, the blade pitch angle controller optimizes the pitch angle to capture the maximum wind power. When the wind speed is higher than its rated value, the pitch angle controller will be activated, and the output power of DFIG is kept at its rated value by adjusting the pitch angle. Therefore, the pitch angle is selected as a clustering indication.

3) ROTOR ANGULAR VELOCITY

According to the power characteristic curve of wind turbine, the relationship between the output power and the angular velocity of the wind turbine is expressed as follows:

$$P_m \propto \omega_m^3 \tag{6}$$

The shaft model represented by a two-mass model is expressed as follows:

$$\frac{d\theta_s}{dt} = \omega_m - \omega_g \tag{7}$$

where ω_m and ω_g are the angular velocity of wind turbine and generator, respectively, θ_s is the shaft torsion angle.

In (6) and (7), the output power of wind turbine also has a relationship with rotor angular velocity. Therefore, as a clustering indication, the rotor angular velocity of generator can reflect the operating characteristics of DFIGs.

4) ROTOR CURRENT

When the stator-flux orientation is used for the RSC control, the decoupling control of the active power and reactive power

will be realized, and they can be expressed as follows:

$$\begin{cases} P_s = u_s i_{qs} = \dfrac{L_m}{L_s} u_s i_{qr} \\ Q_s = -u_s i_{ds} = \dfrac{\psi_s}{L_s} u_s - \dfrac{L_m}{L_s} u_s i_{dr} \end{cases} \tag{8}$$

where u_s is the stator voltage, i_{dr} and i_{qr} are rotor currents in d-axis and q-axis, respectively, L_s is the self-induction of stator, and L_m is the mutual induction of stator and rotor.

Accordingly, i_{dr} and i_{qr} can control the reactive and active power on the stator side, respectively, for the decoupling control of active and reactive power. Since the rotor side power of DFIG is small (up to 30% of the total), the stator side power is considered as the main factor in determining the output power. In other words, the output power of DFIG is reflected in the rotor current i_{dr} and i_{qr}.

5) REAL-TIME POWERS

The performance of the equivalent model is to make the corresponding DFIG output characteristics at grid-connection point consistent with those before the equivalence. And the real-time active power and reactive power are the key representatives of the DFIG output characteristics. Furthermore, the real-time powers can reflect indirectly the performance of wind speed, rotor current and other system operating characteristics. Therefore, the real-time powers are selected as clustering indications.

Accordingly, the comprehensive indicators consisting of wind speed, pitch angle, rotor angular velocity, rotor current and real-time powers are selected as clustering indicators, which could distinguish different operating characteristics of DFIGs in our analyses.

D. COLLECTION OF CLUSTERING INDICATORS

After determining the selection of the clustering indicators, the clustering indications data of each DFIG are collected, including the following steps:

1) Establish the detailed model of wind farm on the PSCAD/EMTDC simulation platform based on the network topology and parameters of wind farm.
2) Read wind speed information.
3) Set the running time and complete the transient simulation of the detailed model.
4) Collect the pitch angle, rotor angular velocity, stator current and real-time powers at steady state.

III. EQUIVALENT PARAMETERS AGGREGATION

A. EQUIVALENT WIND SPEED

In order to ensure the same output power of the wind farm before and after equivalence, the equivalent wind speed is obtained by calculating the average active power of DFIGs in the same group, and it is represented as follows:

$$v_{eq} = f^{-1}\left(\frac{1}{n}\sum_{i=1}^{n} f(v_i)\right) \tag{9}$$

where n is the number of DFIGs in the same group. f is the fitting function of the wind speed power curve.

B. EQUIVALENT PARAMETER OF WIND POWER SYSTEM

Equivalent system parameters are obtained by using the weighted average method. The weighted coefficients and equivalent system parameters are obtained in (10) and (11).

$$\theta_i = \frac{S_i}{\sum_{i=1}^{\mathrm{m}} S_i} \tag{10}$$

$$\begin{cases} Z_{eq} = \sum_{i=1}^{n} (\theta_i Z_i),\ H_{eq} = \sum_{i=1}^{n} (\theta_i H_i) \\ D_{eq} = \sum_{i=1}^{n} (\theta_i D_i),\ K_{eq} = \sum_{i=1}^{n} (\theta_i K_i) \\ Z_{T\_eq} = \sum_{i=1}^{n} (\theta_i Z_{T\_i}),\ S_{eq} = \sum_{i=1}^{n} S_i \end{cases} \tag{11}$$

where m is the total number of DFIGs in the wind farm. Z and Z_T are the impedance parameter of generator and transformer, respectively. H, D, K are the inertia constant, damping coefficient and stiffness coefficient, respectively. S is the capacity of the DFIG.

C. EQUIVALENT PARAMETER OF COLLECTING LINE

The equivalent impedance parameter of collector line can be represented as follows:

$$Z_{L\_eq} = \frac{\sum_{i=1}^{m}\left(\sum_{k=1}^{i}\left(Z_{L\_k}\sum_{j=k}^{n} P_j\right)P_i\right)}{\left(\sum_{i=1}^{n} P_i\right)^2} \tag{12}$$

where Z_L is the impedance parameter of the cable line.

Through the equivalence of impedance parameters, it can be ensured that the voltage loss on the collector line is consistent before and after the equivalence.

D. ERROR ANALYSIS OF EQUIVALENT MODEL

In order to compare the accuracy of different equivalent methods, the average power deviation is usually used as the evaluation index of the equivalent model, and the active average deviation amount E_P and the reactive average deviation amount E_Q are defined as follows:

$$E_P = \frac{\int_{t_1}^{t_2} \left|P_{eq}(t) - P(t)\right| dt}{\int_{t_1}^{t_2} |P(t)| dt} \tag{13}$$

$$E_Q = \frac{\int_{t_1}^{t_2} \left|Q_{eq}(t) - Q(t)\right| dt}{\int_{t_1}^{t_2} |Q(t)| dt} \tag{14}$$

where P and Q are active and reactive power of the detailed wind farm model, respectively.

IV. CASE STUDY

The detailed model of a wind farm consisting of 16 × 5 MW DFIGs is set up on the PSCAD/EMTDC simulation platform. Each DFIG is connected to the point of common coupling (PCC) through a 0.69kV/35kV step-up transformer, and the power output is delivered to the power grid via a 35kV/230 kV step-up transformer. The main parameters of DFIG are shown in Table 1, and the input wind speeds of each DFIG are shown in Table 2. The clustering indicator data of DFIGs are shown in Table 3, which collected in the detailed model simulation.

TABLE 1. Parameters of DFIG

Parameters	Symbol	Value	Unit
Rated power	P_N	5	MW
Rated frequency	f_s	60	*Hz*
Rated PCC voltage	V_{PCC}	33	kV
Rated stator voltage	V_s	0.9	kV
Rated rotor voltage	V_r	0.69	kV
Rated DC link voltage	V_{dc}	1.45	kV
Rated rotating speed	ω_g	376.99	rad/s
DC link capacitor	C_{dc}	7500	μF
Maximum operating slip	s	0.3	/
Stator leakage inductance	L_s	0.100	*p.u.*
Rotor leakage inductance	L_r	0.110	*p.u.*
Magnetizing inductance	L_m	4.5	*p.u.*
Stator resistance	R_s	0.0054	*p.u.*
Rotor resistance	R_r	0.00607	*p.u.*
Inertia constant	H	6	s

TABLE 2. Input wind speeds of each DFIG

Number	Wind speed	Number	Wind speed
1	10.56	9	9.58
2	8.95	10	11.35
3	11.57	11	10.7
4	10.31	12	8.82
5	9.7	13	9.06
6	10.01	14	9.81
7	9.89	15	10.25
8	9.37	16	10.41

A. VERIFICATION OF CLUSTERING METHODS

According to the input wind speeds shown in Table 2, the wind farm is grouped using the ABC-KM algorithm proposed in this paper and the existing KM algorithm, where the wind farm is equivalent to 4 DFIGs. The clustering results of the two algorithms are shown in Tables 4 and 5, respectively. In order to verify the effectiveness of the dynamic equivalence method proposed in this paper, we present the comparative analyses of dynamic response characteristics at the grid-connection point of detailed model, multi-machine equivalent model with existing KM algorithm, and multi-machine equivalent model with ABC-KM algorithm. We present the steady-state and dynamic-state results considering wind speed disturbances and short-circuit faults.

TABLE 3. Clustering indicator data of DFIGs

Wind speed	Pitch angle	Rotor angular velocity	Active power	Reactive power	Rotor current in d-axis	Rotor current in q-axis
10.56	0	1.2215	4.9994	-0.1224	-0.0992	0.1937
8.95	0	1.2046	3.3409	-0.0859	0.0288	0.1726
11.57	4.3407	1.2171	4.9903	-0.1232	-0.1427	0.1870
10.31	0	1.2176	4.9923	-0.1252	-0.1452	0.1865
9.7	0	1.2102	4.2577	-0.1034	-0.0332	0.1857
10.01	0	1.2135	4.6770	-0.1141	-0.0900	0.1868
9.89	0	1.2125	4.5091	-0.1107	-0.0800	0.1840
9.37	0	1.2080	3.8328	-0.0962	-0.0153	0.1773
9.58	0	1.2091	4.1014	-0.1002	-0.0183	0.1843
11.35	3.9134	1.2154	4.9921	-0.1212	-0.1205	0.1899
10.7	0	1.2247	4.9968	-0.1253	-0.1095	0.1919
8.82	0	1.2037	3.1949	-0.0845	0.0487	0.1718
9.06	0	1.2050	3.4680	-0.0877	0.0334	0.1772
9.81	0	1.2118	4.4016	-0.1080	-0.0807	0.1818
10.25	0	1.2165	4.9926	-0.1246	-0.1492	0.1860
10.41	0	1.2195	4.9930	-0.1259	-0.1468	0.1865

1) STEADY-STATE SIMULATION

The wind speed shown in Table 2 is adopted as the input wind speed of wind farm at steady state. The simulation results at the grid-connection point are shown in Figure 3.

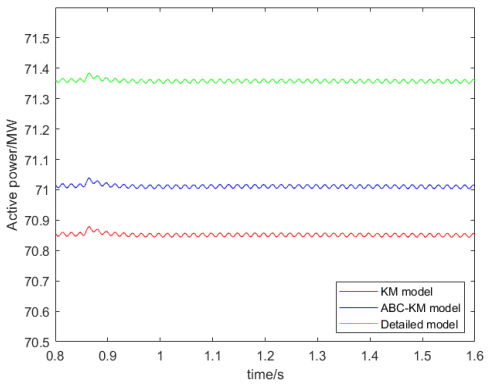

(a) Response curve of active power

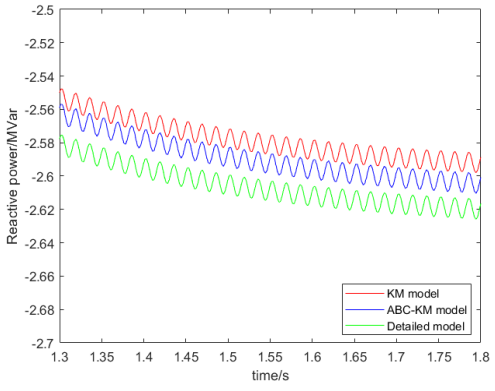

(b) Response curve of reactive power

FIGURE 3. Response curves of wind farm in the steady state.

TABLE 4. Clustering result with ABC-KM algorithm

Number of clusters	Number of DFIGs
1	1, 4, 6, 11, 15, 16
2	2, 12, 13
3	3, 10
4	5, 7, 8, 9, 14

TABLE 5. Clustering result with existing KM algorithm

Number of clusters	Number of DFIGs
1	1, 4, 11, 15, 16
2	2, 8, 12, 13
3	3, 10
4	5, 6, 7, 9, 14

2) WIND SPEED DISTURBANCE

Based on the basic wind speed, the wind gust disturbance is added starting at 0.8s, ending at 1.8s, and the peak velocity is 1m/s. The power simulation results at the grid-connection point are shown in Figure 4.

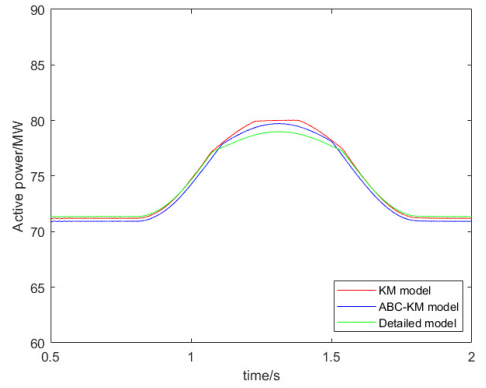

(a) Response curve of active power

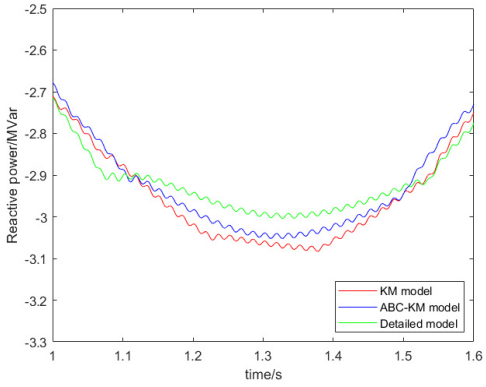

(b) Response curve of reactive power

FIGURE 4. Response curves of wind farm in the wind speed disturbance.

3) GRID FAULT

In order to compare the equivalent effects of different equivalent models under a short-circuit grid fault, we assume that the fault occurs at 1s, is cleared at 1.3s, and the voltage sag amplitude is 50%. The power simulation results at the grid-connection point are shown in Figure 5.

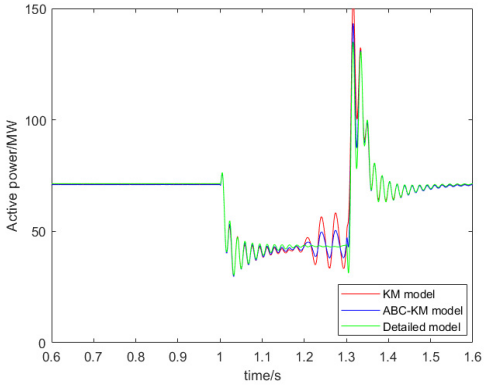

(a) Response curve of active power

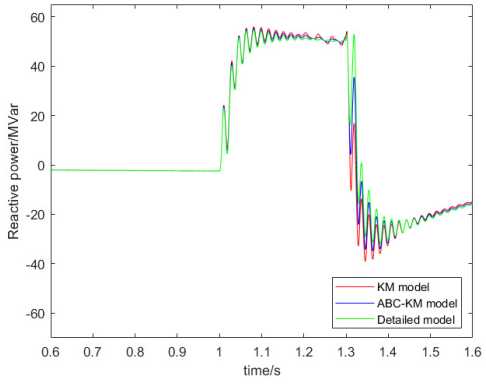

(b) Response curve of reactive power

FIGURE 5. Response curves of wind farm in the grid fault.

It can be seen from Figures 3 to 5 that the power dynamic responses of the multi-machine equivalent model using the proposed method are much closer to those of the detailed model at the steady-state and dynamic-state cases, as compared with the equivalent model based on the KM algorithm.

In Table 6, we use the detailed model as the benchmark to analyze the errors in the two multi-machine equivalent models, and present the results for the proposed ABC-KM and existing KM algorithms. The results show that, compared with the existing KM algorithm, the power dynamic responses of multi-machine equivalent model with the ABC-KM algorithm are more consistent with those of the detailed model at steady-state and dynamic-state cases.

B. VERIFICATION OF CLUSTERING INDICATORS

In order to further prove the effectiveness of the clustering indicators, using the ABC-KM algorithm, the wind farm is grouped according to the wind speed and the proposed comprehensive indicators shown in Table 3. The clustering results of the comprehensive indicators and wind speed are shown in Tables 7 and 8.

TABLE 6. Error comparison for different equivalent methods

System operation status	ABC-KM algorithm		KM algorithm	
	Active power error	Reactive power error	Active power error	Reactive power error
Steady state	0.49%	0.78%	0.70%	1.16%
Wind speed disturbance	0.51%	1.12%	0.78%	1.32%
Grid fault	0.55%	0.83%	0.84%	1.27%

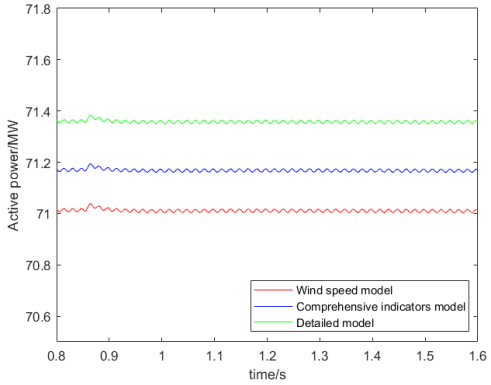

(a) Response curve of active power

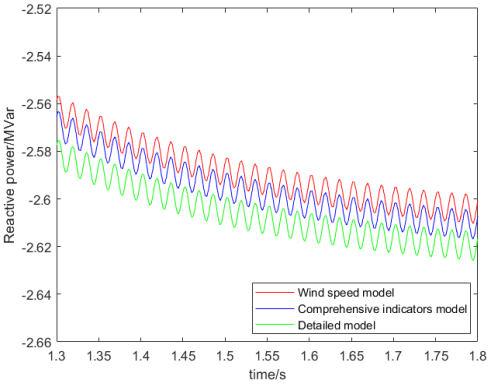

(b) Response curve of reactive power

FIGURE 6. Response curves of wind farm in the steady state.

TABLE 7. Clustering result by comprehensive indicators

Number of clusters	Number of DFIGs
1	1, 4, 6, 11, 15, 16
2	2, 12, 13
3	3, 10
4	5, 7, 8, 9, 14

TABLE 8. Clustering result by wind speed

Number of clusters	Number of DFIGs
1	1, 4, 11, 15, 16
2	2, 12, 13
3	3, 10
4	5, 6, 7, 8, 9, 14

1) STEADY-STATE SIMULATION

In order to verify the effectiveness of clustering indicators at steady state, the power simulation results at the grid-connection point are shown in Figure 6.

2) WIND SPEED DISTURBANCE

Based on the basic wind speed, the wind gust disturbance is added starting at 0.8s, ending at 1.8s, and the peak velocity is 1m/s. In this case, the power simulation results at the grid-connection point are shown in Figure 7.

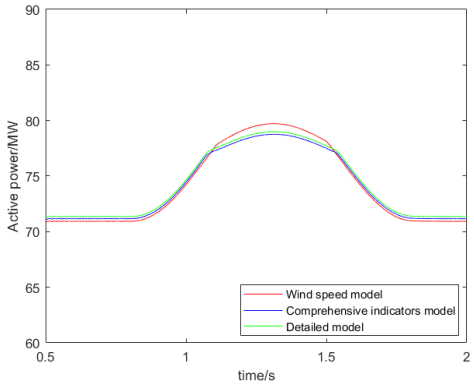

(a) Response curve of active power

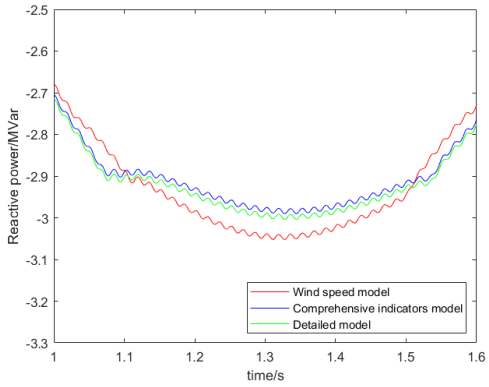

(b) Response curve of reactive power

FIGURE 7. Response curves of wind farm in the wind speed disturbance.

3) GRID FAULT

We assume that a short-circuit grid fault occurs at 1s, is cleared at 1.3s, and the voltage sag amplitude is 50%. And the power simulation results at the grid-connection point are shown in Figure 8.

It can be seen from Figures 6 to 8 that the power dynamic responses of the multi-machine equivalent model based on the wind speed present a large error in comparison with those of the detailed model. The power dynamic responses of the multi-machine equivalent model based on the comprehensive indicators are consistent with those of the detailed model. To analyze the errors in the multi-machine equivalent model based on the comprehensive indicators and wind speed, we use the detailed model as the benchmark to analyze, and present the results in Table 9. Accordingly, the power dynamic responses of multi-machine equivalent model based on the comprehensive indicators are more closely related to those of the detailed model at steady-state and dynamic-state cases.

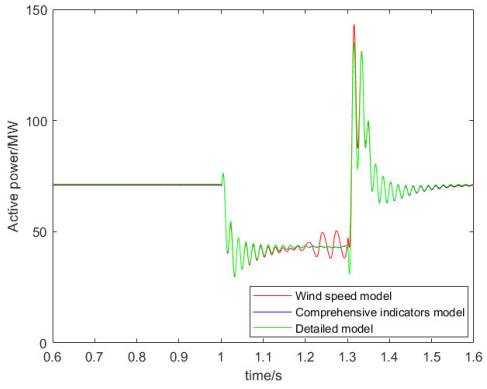

(a) Response curve of active power

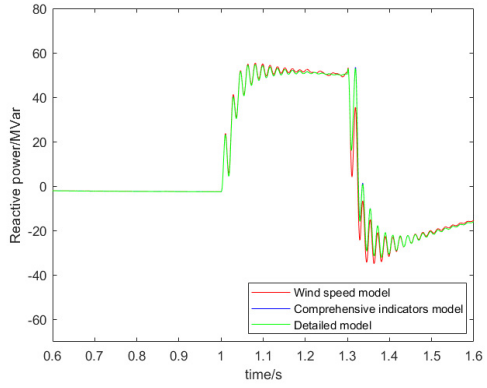

(b) Response curve of reactive power

FIGURE 8. Response curves of wind farm in the grid fault.

TABLE 9. Error comparison for different clustering indicators

System operation status	Comprehensive indicators model		Wind speed model	
	Active power error	Reactive power error	Active power error	Reactive power error
Steady-state	0.28%	0.52%	0.49%	0.78%
Wind speed disturbance	0.26%	0.45%	0.51%	1.12%
Grid fault	0.27%	0.44%	0.55%	0.83%

C. SIMULATION TIME COMPARISONS

The proposed simulations are carried out on a personal computer Intel (R) Core (TM), i7-6700HQ, Quad-core CPU @ 2.60 GHz, 16 GB of RAM. The simulation times for different equivalent methods are shown in Table 10. It can be seen from Table 10 that the simulation times corresponding to the two kinds of multi-machine equivalent models are very close. However, compared to the detailed model, the simulation time of the multi-machine equivalent model is reduced by about 98%.

In summary, considering the steady-state and dynamic-state, the power responses of the multi-machine equivalent model with ABC-KM algorithm are much closer to those of the detailed model as compared to those of the equivalent model with the existing KM algorithm. And the power responses of multi-machine equivalent model based on the comprehensive indicators are more consistent with those of the detailed model as compared with the equivalent model based on the wind speed. Furthermore, compared with the detailed model, the dynamic equivalent model is simplified and the calculation time is reduced significantly.

TABLE 10. Simulation time comparison for different models

Model	Simulation time (s)
Detailed model	34200
Multi-machine equivalent model with ABC-KM	670
Multi-machine equivalent model with KM	670

V. CONCLUSION

In order to meet the practical engineering requirement, a multi-machine dynamic equivalence method for wind farm with DFIGs is proposed in this paper. First, the artificial bee colony with k-means (ABC-KM) algorithm is proposed to improve the effectiveness of clustering. Second, the comprehensive indicators composed of wind speed, pitch angle, rotor angular velocity, rotor current, real-time active and reactive power are selected as clustering indicators. The wind farm with DFIGs is divided into groups and DFIGs in which each group is represented by single DFIG using equivalent parameters. Finally, the multi-machine dynamic equivalent model of wind farm with DFIG is established and studied on the PSCAD/EMTDC simulation platform according to the aggregation of equivalent parameters.

The simulation results demonstrate that multi-machine equivalent model established in this paper can reflect dynamic response characteristics of wind farm with DFIG effectively. At the same time, compared with the detailed model, the multi-machine dynamic equivalent model is simplified and the calculation time is reduced significantly.

REFERENCES

[1] S. R. Etesami, W. Saad, N. B. Mandayam, and H. V. Poor, "Stochastic games for the smart grid energy management with prospect prosumers," *IEEE Trans. Autom. Control*, vol. 63, no. 8, pp. 2327–2342, Aug. 2018.

[2] H. Wang, Y. Liu, B. Zhou, C. Li, G. Cao, N. Voropai, and E. Barakhtenko, "Taxonomy research of artificial intelligence for deterministic solar power forecasting," *Energy Convers. Manage.*, vol. 214, Jun. 2020, Art. no. 112909.

[3] D. Xu, Q. Wu, B. Zhou, C. Li, L. Bai, and S. Huang, "Distributed multi-energy operation of coupled electricity, heating and natural gas networks," *IEEE Trans. Sustain. Energy*, early access, Dec. 23, 2020, doi: 10.1109/TSTE.2019.2961432.

[4] H. Wang, Z. Lei, X. Zhang, B. Zhou, and J. Peng, "A review of deep learning for renewable energy forecasting," *Energy Convers. Manage.*, vol. 198, Oct. 2019, Art. no. 111799.

[5] L. M. Fernández, F. Jurado, and J. R. Saenz, "Aggregated dynamic model for wind farms with doubly fed induction generator wind turbines," *Renew. Energy*, vol. 33, no. 1, pp. 129–140, Jan. 2008.

[6] W. Li, P. Chao, X. Liang, J. Ma, D. Xu, and X. Jin, "A practical equivalent method for DFIG wind farms," *IEEE Trans. Sustain. Energy*, vol. 9, no. 2, pp. 610–620, Apr. 2018.

[7] J. Qi, P. Chao, X. Jin, and W. Li, "Dynamic equivalent modeling of direct-drive PMSG wind farms based on the transient active power response characteristics," in *Proc. IEEE 8th Int. Power Electron. Motion Control Conf.*, Hefei, China, May 2016, pp. 2925–2930.

[8] H. Kim, C. Singh, and A. Sprintson, "Simulation and estimation of reliability in a wind farm considering the wake effect," *IEEE Trans. Sustain. Energy*, vol. 3, no. 2, pp. 274–282, Apr. 2012.

[9] J. Tian, D. Zhou, C. Su, Z. Chen, and F. Blaabjerg, "Reactive power dispatch method in wind farms to improve the lifetime of power converter considering wake effect," *IEEE Trans. Sustain. Energy*, vol. 8, no. 2, pp. 477–487, Apr. 2017.

[10] M. Liu, W. Pan, Y. Zhang, K. Zhao, S. Zhang, and T. Liu, "A dynamic equivalent model for DFIG-based wind farms," *IEEE Access*, vol. 7, pp. 74931–74940, May 2019.

[11] S. Chen, C. Wang, H. Shen, N. Gao, L. Zhu, and H. Lan, "Dynamic equivalence for wind farms based on clustering algorithm," *Proc. CSEE*, vol. 32, no. 4, pp. 11–19, Feb. 2012.

[12] D.-E. Kim and M. A. El-Sharkawi, "Dynamic equivalent model of wind power plant using parameter identification," *IEEE Trans. Energy Convers.*, vol. 31, no. 1, pp. 37–45, Mar. 2016.

[13] Z. Zhao, P. Yang, Z. Xu, and X. Yin, "Dynamic equivalent modeling of wind farm with double fed induction wind generator based on operating data," in *Proc. 5th Int. Conf. Power Electron. Syst. Appl.*, Hong Kong, Dec. 2013, pp. 1–6.

[14] Q. Zhu, P. Han, M. Ding, X. Zhang, and W. Shi, "Probabilistic equivalent model for wind farms based on clustering-discriminant analysis," *Proc. CSEE*, vol. 34, no. 28, pp. 4770–4780, Oct. 2014.

[15] W. Teng, X. Wang, Y. Xiao, and W. Shi, "Dynamic multi-turbine multi-state model of wind farm based on historical wind data," in *Proc. IEEE PES Asia–Pacific Power Energy Eng. Conf. (APPEEC)*, Hong Kong, Dec. 2014, pp. 1–5.

[16] M. Ali, I.-S. Ilie, J. V. Milanovic, and G. Chicco, "Wind farm model aggregation using probabilistic clustering," *IEEE Trans. Power Syst.*, vol. 28, no. 1, pp. 309–316, Feb. 2013.

[17] J. Zou, C. Peng, H. Xu, and Y. Yan, "A fuzzy clustering algorithm-based dynamic equivalent modeling method for wind farm with DFIG," *IEEE Trans. Energy Convers.*, vol. 30, no. 4, pp. 1329–1337, Dec. 2015.

[18] W. Teng, X. Wang, Y. Meng, and W. Shi, "An improved support vector clustering approach to dynamic aggregation of large wind farms," *CSEE J. Power Energy Syst.*, vol. 5, no. 2, pp. 215–223, Jun. 2019.

[19] P. Wang, Z. Zhang, Q. Huang, N. Wang, X. Zhang, and W. Lee, "Improved wind farm aggregated modeling method for large-scale power system stability studies," *IEEE Trans. Power Syst.*, vol. 33, no. 6, pp. 6332–6342, Nov. 2018.

[20] Y. Jin and P. Ju, "Dynamic equivalent modeling of FSIG based wind farm according to slip coherency," in *Proc. Int. Conf. Sustain. Power Gener. Supply*, Nanjing, China, Apr. 2009, pp. 1–7.

[21] X. Huang, Y. Ye, and H. Zhang, "Extensions of kmeans-type algorithms: A new clustering framework by integrating intracluster compactness and intercluster separation," *IEEE Trans. Neural Netw. Learn. Syst.*, vol. 25, no. 8, pp. 1433–1446, Aug. 2014.

[22] T. Lei, M. Ozakturk, and M. Barnes, "Doubly-fed induction generator wind turbine modelling for detailed electromagnetic system studies," *IET Renew. Power Gener.*, vol. 7, no. 2, pp. 180–189, Mar. 2013.

[23] L. Yang, X. Sun, L. Peng, X. Yao, and T. Chi, "An agent-based artificial bee colony (ABC) algorithm for hyperspectral image endmember extraction in parallel," *IEEE J. Sel. Topics Appl. Earth Observ. Remote Sens.*, vol. 8, no. 10, pp. 4657–4664, Jul. 2015.

XIAOHUI WANG (Graduate Student Member, IEEE) was born in Xiaoyi, Shanxi, China, in 1996. He received the B.E. degree in electrical engineering from Zhengzhou University, Zhengzhou, China, in 2018. He is currently pursuing the M.S. degree with the College of Electrical and Information Engineering, Hunan University, Changsha, China. His major research interests include wind turbine and wind farm modeling.

HAO YU was born in Hubei, China, in 1986. He received the master's degree in power system and automation from North China Electric Power University, Beijing, China, in 2012. He is currently a Power Grid Planning Engineer with the Grid Planning and Research Centre, Guangdong Power Grid Company, Ltd., Guangzhou, China. His major research interests include power system planning and reliability.

YONG LIN was born in Guangan, Sichuan, China, in 1973. He received the master's degree in power electronics and power drives from North China Electric Power University, Beijing, China, in 2001. He is currently a Power Grid Planning Senior Engineer with the Grid Planning and Research Centre, Guangdong Power Grid Company, Ltd., Guangzhou, China. His major research interests include power system planning and reliability.

ZHEMENG ZHANG (Graduate Student Member, IEEE) was born in Ningbo, Zhejiang, China, in 1997. He received the B.E. degree in electrical engineering from the Changsha University of Science and Technology, Changsha, China, in 2019. He is currently pursuing the M.S. degree with the College of Electrical and Information Engineering, Hunan University, Changsha, China. His major research interests include wind power model and power system stability analysis.

XIANFU GONG was born in Xianning, Hubei, China, in 1987. He received the master's degree in power system and automation from Zhejiang University, Hangzhou, China, in 2012. He is currently a Power Grid Planning Engineer with Guangdong Power Grid Development Research Institute Company, Ltd., Guangzhou, China. His major research interests include power system planning and reliability.